Journal of Biomolecular NMR, **14:** 357–368, 1999.
KLUWER/ESCOM

The effect of helix-coil transition on backbone ^{15}N NMR relaxation of isolated transmembrane segment (1–36)-bacteriorhodopsin

Dmitry M. Korzhnev[a], Vladislav Yu. Orekhov[a,b] & Alexander S. Arseniev[a,*]
[a] *Shemyakin and Ovchinnikov Institute of Bioorganic Chemistry, Russian Academy of Sciences, Ul. Miklukho-Maklaya 16/10, 117871 Moscow, Russia;* [b] *Biochemistry and Biophysics, Lundberg Laboratory, Göteborg University, Box 462, SE 405 30 Göteborg, Sweden*

Received 13 April 1999; Accepted 24 June 1999

Key words: α-helix propensities of amino acids, discrete jumps, helix-coil kinetics, membrane proteins, transmembrane α-helix

Abstract

In this paper we develop a motional model of isolated transmembrane segment 1–36 bacteriorhodopsin (BR) in a weakly polar organic mixture. The model is based on the statistical mechanics theory [Lifson, S. and Roig, A. (1961) *J. Chem. Phys*., **34**, 1963–1974] and represents the dynamics of 1–36BR as an interconversion between a limited number of intermediates of α-helix – random coil transition. The equilibrium parameters of helix-coil transition were selected by the comparison of calculated profiles of mean residual helicity of 1–36BR with the available experimental data. The kinetic modeling of the helix-coil transition was used for calculation of the correlation functions of internal motions of the backbone NH vectors. The calculated correlation functions are multiexponential and consist of two groups of exponential terms: 'fast' (pico–nanoseconds) and 'slow' (sub-microseconds). The decay of the correlation functions on the pico–nanosecond time-scale was used for qualitative estimates of NMR observable order parameters of the backbone NH vectors. The calculated order parameters are in good correspondence with the experimental values obtained from 'model-free' analysis of ^{1}H-^{15}N NMR relaxation data [Orekhov et al. (1999) *J. Biomol. NMR*, **14**, 345–356]. Low and uniform (over the peptide) order parameters of nanosecond time-scale motions ($S_s^2 \sim 0.5$–0.6) are accounted for by the exchange between kinked states with several α-helical regions within 1–36BR. These states are caused by the presence of helix breaking residues Gly and Thr in the central part of 1–36BR.

Introduction

It is widely recognized that isolated α-helices in solution exist as a number of exchanging species – intermediates of helix-coil transition. The kinetics of helix-coil transition was extensively studied by numerous experimental and theoretical methods. Ultrasonic absorption and dielectric relaxation experiments, performed on long α-helical homopolymers (Schwartz, 1965; Schwartz and Seelig, 1968), as well as modern laser-induced temperature jump studies of short water-soluble α-helices (Williams et al., 1996; Thompson et al., 1997) show that helix-coil transition occurs on time-scales from tens or hundreds of nanoseconds to microseconds. The theoretical consideration suggests that the relaxation spectrum of helix-coil transition is extremely broad (Schwartz, 1965, 1968). Recent kinetic modeling of a short alanine-based α-helix (Thompson et al., 1997) shows that the wide spectrum of relaxation times of helix-coil transition clusters at two distinct groups: 'slow', i.e. hundreds of nanoseconds, and 'fast', pico- to nanoseconds. In principle, the processes associated with the pico–nanosecond part of the helix-coil relaxation spectrum can influence ^{1}H-^{15}N NMR relaxation.

Our NMR relaxation study of isolated transmembrane segment 1–36 bacteriorhodopsin (BR) in a membrane-mimicking chloroform/methanol 1:1 mix-

*To whom correspondence should be addressed. E-mail: aars@nmr.ru.

ture reveals substantial internal mobility of the α-helix on the nanosecond time scale with low and *uniform* (over the peptide) order parameters ($S_s^2 \sim 0.5$–0.6) of backbone ^{1}H-^{15}N vectors (Orekhov et al., 1999). The results of molecular dynamics (MD) simulations of 1–36BR in weakly polar medium (Korzhnev et al., 1999) suggest that low order parameters of backbone ^{1}H-^{15}N vectors are presumably caused by kinked states of the α-helix, arising due to the formation of propagated distortions with π-helical hydrogen bonds in the central part of the peptide. However, MD simulations cannot provide the estimates of the order parameters of nanosecond motions, because the lengths of the trajectories are not sufficient for the adequate sampling of conformational space. In this paper we develop a simple motional model of 1–36BR for the interpretation of backbone ^{1}H-^{15}N NMR relaxation data. The model is based on statistical mechanics theory of α-helix-random coil transition (Lifson and Roig, 1961). The dynamics of 1–36BR is represented as an interconversion between a relatively small number of helix-coil intermediates. The influence of this process on NMR relaxation is treated within the frame of the discrete jump model of internal motions (King et al., 1978; King and Jardetzky, 1978; Wittebort and Szabo, 1978; Tropp, 1980).

Theory and methods

Lifson-Roig statistical mechanics theory of helix-coil transition

The Lifson–Roig theory was selected from two alternative statistical mechanics theories of helix-coil transition (Zimm and Bragg, 1959; Lifson and Roig, 1961) for the analysis of 1–36BR, because this theory is better adapted for the analysis of the helix formation by short heteropeptides (see Doig et al., 1994). In the Lifson–Roig theory the polypeptide chain is represented as a one-dimensional sequence of residues adopting one of two possible conformations – helix or coil. Thus, the conformational space of the peptide of N residues consists of 2^N states. The residue is assumed to the in helical (h) conformation if its φ and ψ backbone dihedral angles are around $-57\,^\circ$ and $-47\,^\circ$, respectively. The backbone dihedral angles, located in the remaining area of the (φ, ψ) map, correspond to the coil (c) conformation.

There are several rules to define the statistical weights of the states of the polypeptide chain: (i) The statistical weight of each state is a product of the statistical weights of the residues in particular conformations. (ii) The statistical weight of each residue is determined by its own conformation and by the conformations of its nearest neighbors (so-called nearest neighbor cooperativity). In the Lifson–Roig theory the weight of a residue in a coil state is always equal to $u \equiv 1$. The weight of a residue in α-helical state depends on its type and on the conformations of two adjacent residues. The weight w is assumed if both neighbors of the helical residue are in helical conformation. It is notable that w-weighting of residue i is the necessary condition for the formation of an α-helical hydrogen bond between the CO group of residue $i-2$ and the NH group of residue $i+2$. The number of w-weighted residues is assumed to be equal to the number of α-helical hydrogen bonds formed by the peptide. The terminal helical residues, and the residues adjacent to the coil region have the weights v. Thus, for example, the state 'chhhcc' of the polypeptide chain has the statistical weight uvw_3vuu (assuming that w depends on residue type and v is the same for all residues). For evaluation of the statistical weights of the states of 1–36BR the constants v and w were calculated from the conventional Zimm–Bragg nucleation parameter σ and propagation constants s (otherwise called helix propensities of amino acids) using the relationships of Qian and Schellman (1992):

$$s_i = \frac{w_i}{1+v} \qquad \sigma = \frac{v^2}{(1+v)^4} \tag{1}$$

The sum of the statistical weights of the states is the quantity of general importance referred to as the *configuration partition function*. The partition function provides a simple way for calculations of the ensemble average properties, related to the values of experimentally observable parameters. In particular, the probability $p(w_i)$ to form an $i-2 \rightarrow i+2$ hydrogen bond (w-weighting of residue i) and the probability $p(v_i)$ for residue i to terminate the helix region (v-weighting of residue i) can be calculated as:

$$p(w_i) = \frac{\partial(ln\,Q)}{\partial(ln\,w_i)} \qquad p(v_i) = \frac{\partial(ln\,Q)}{\partial(ln\,v_i)} \tag{2}$$

where Q is the partition function.

A set of relative helix propensities (s) and a nucleation parameter (σ), appropriated for modeling of 1–36BR in a weakly polar organic mixture, were selected using the comparison of the calculated profiles of mean residual helicity (Equation 2) with (i) spatial structure, (ii) data on the deuterium exchange of the backbone amides of 1–36BR in chloroform/methanol 1:1 mixture (Pervushin et al., 1992) and (iii) results

Table 1. Relative helix propensities for 1–36BR residues

Residue	Relative helix propensities	
	Chakrabartty and Baldwin, 1995	Park et al., 1993
pGln1[a]	0.53	0.58
Ala2	1.54	1.81
Gln3	0.53	0.58
Ile4	0.42	0.43
Thr5	0.13	0.18
Gly6	0.05	0.05
Arg7	1.10	1.83
Pro8	0.001	0.001
Glu9	0.63	1.00
Trp10	0.29–0.36[b]	0.58
Ile11	0.42	0.43
Trp12	0.29–0.36[b]	0.58
Leu13	0.92	1.03
Ala14	1.54	1.81
Leu15	0.92	1.03
Gly16	0.05	0.05
Thr17	0.13	0.18
Ala18	1.54	1.81
Leu19	0.92	1.03
Met20	0.60	0.79
Gly21	0.05	0.05
Leu22	0.92	1.03
Gly23	0.05	0.05
Thr24	0.13	0.18
Leu25	0.92	1.03
Tyr26	0.37–0.50[b]	0.43
Phe27	0.28	0.79
Leu28	0.92	1.03
Val29	0.22	0.18
Lys30	0.78	1.25
Gly31	0.05	0.05
Met32	0.60	0.79
Gly33	0.05	0.05
Val34	0.22	0.18
Ser35	0.26	0.28
Asp36[a]	0.29	0.24

[a]The terminal amino acid residues were not considered in the calculations with the Lifson–Roig theory since these residues are not flanked by a peptide group on both sides.
[b] The maximal value from the range was selected for the calculations.

of the MD simulations of 1–36BR in the same system (Korzhnev et al., 1999). Several sets of relative helix propensities of amino acids were tested (Table 1). Relative helix propensities were scaled to obtain a mean helix content of 0.6 in the position of the α-helix in chloroform/methanol 1:1 mixture (residues 8–32) (Pervushin et al., 1992). This helix content corresponds to averaged populations of α-helical hydrogen bonds in the 8–32 region observed in the MD simulations of 1–36BR in a weakly polar medium (Korzhnev et al., 1999). The calculations were performed for three values of the helix nucleation parameter ($\sigma = 10^{-4}$, 10^{-3} and 10^{-2}), assumed to be the same for all amino acids of 1–36BR. This assumption is valid for amino acids with a chemically equivalent backbone (Scholtz and Baldwin, 1992).

Kinetic model of helix-coil transition

For a peptide of N residues the exchange between 2^N helix-coil intermediates can be described in terms of the system of first-order rate equations:

$$\frac{d}{dt}p_i(t) = \sum_{j=1(i\neq j)}^{2^N} \left(p_j(t)k_{ji} - p_i(t)k_{ij}\right) \qquad (3)$$

where p_i is the population of the *i*-th state of the polypeptide chain and k_{ij} is the rate constant of the transition between the *i*-th and *j*-th states. In matrix notation the system of rate equations 3 can be written as

$$\mathbf{p}'(t) = \mathbf{A}\mathbf{p}(t) \qquad (4)$$

where **A** is the transition rate matrix with the elements $A_{ij} = k_{ji}(i \neq j)$ and $\mathbf{p}(t) = \left(p_1(t), \ldots, , p_{2^N}(t)\right)^T$ is the vector of populations. The elements of **p**(*t*) and **A** satisfy the conditions

$$\sum_{i=1}^{2^N} A_{ij} = 0 \qquad \sum_{i=1}^{2^N} p_i(t) = 1 \qquad (5)$$

and the condition of microscopic reversibility

$$A_{ij}p_j^* = A_{ji}p_i^* \qquad (6)$$

where p_i^* and p_j^* are the equilibrium populations of the *i*-th and *j*-th states of the polypeptide chain, obtained from Equation 4, assuming $\mathbf{p}'(t) = 0$. The dimensionality of the rate matrix **A** does not exceed $2^N - 1$. Therefore, the matrix has at least one zero eigenvalue. The condition of microscopic reversibility, Equation 6, ensures that all eigenvalues of the rate matrix are real. The nonzero eigenvalues are negative. The solution of rate equation 4 can be written as:

$$\mathbf{p}(t) = \mathbf{p}^* + \sum_{i=1}^{2^N-1} c_i^{cond} \mathbf{x}_i e^{\lambda_i t} \quad (7)$$

where $\mathbf{p}^*$ is the vector of equilibrium populations and $\mathbf{x}_i$ are the eigenvectors, corresponding to nonzero eigenvalues λ_i of rate matrix **A**. The coefficients c_i^{cond} depend on the initial state of the polypeptide chain and can be calculated from the system of linear equations:

$$\mathbf{p}(0) - \mathbf{p}^* = \sum_{i=1}^{2^N-1} c_i^{cond} \mathbf{x}_i = \mathbf{X}\mathbf{c}^{cond} \quad (8)$$

where **X** is a $(2^N - 1) \times 2^N$ matrix composed from the eigenvectors of the rate matrix **A** and $\mathbf{c}^{cond}$ is the vector of $2^N - 1$ coefficients. The fact that the eigenvalues are real and negative determines the dissipative nature of the process, which is characterized by $2^N - 1$ correlation times $\tau_i = -1/\lambda_i$. Equations 7 and 8 allow to model kinetics of any observable quantity with known relationship between the populations of the states of the polypeptide chain.

Modeling of the kinetics of helix-coil transition requires the knowledge of elements of the rate matrix **A**, characterizing the rates of transitions between the states of the polypeptide chain. The rate matrix was built by following the strategy of Schwartz (1965, 1968). We assume that the transitions between the states, which differ in the conformations of more than one residue, are prohibited, so the corresponding elements of the rate matrix were set to zero. Thus, the number of allowed transitions between the species is limited to the simple processes of helix nucleation (formation of the first helix turn within the coil region) and helix propagation (growth of the unperturbed helix sequence by conversion of a single residue at the helix end). The reaction of coil nucleation (formation of helix breaks) is considered to be a reverse to the reaction of propagation of one of two adjacent helical regions. In general, the description of helix-coil kinetics requires the introduction of a large number of kinetic parameters, characterizing each elementary process. To reduce the number of kinetic parameters we assume that (i) all helix propagation reactions are described by the same rates k_F, (ii) the helix nucleation process is much slower than helix propagation and (iii) the reaction of disappearance of helix nucleus is faster than the reverse reaction of helix propagation. The assumptions (ii) and (iii) determine the ranges of rate constant of helix nucleation and allow to express it in terms of helix propagation rate k_F. For the calculations we select the minimal allowed rates of helix nucleation. The rates of the reverse reactions are always calculated from the rates of forward reactions and the weights of the states of polypeptide chain. The procedure of the selection of the rates of elementary transitions is summarized in Table 2.

Thus, to describe helix-coil kinetics in terms of Lifson–Roig *w* and *v* constants we need only one kinetic parameter: the rate constant of the helix propagation k_F. The values of k_F measured in random copolymers were reviewed by Zana (1975). The rates are in the range of 10^7–$10^{11} s^{-1}$, values of 10^8–$10^9 s^{-1}$ are more probable. The value of $10^8 s^{-1}$ was obtained by Thompson et al. (1997) from the kinetic analysis of a short alanine-based peptide. The results of molecular dynamics simulations of the unfolding of α-helix in water provide somewhat faster rates of the order of 10^{10}–$10^{11} s^{-1}$ (Dagget and Levitt, 1992). In our calculations k_F was set to the value of $10^9 s^{-1}$.

Effect of helix-coil transition on ^1H-^{15}N NMR relaxation

The relaxation of the backbone ^{15}N nucleus in ^{1}H-^{15}N two-spin systems is governed by two dominant mechanisms: (i) the dipole-dipole interactions with the directly attached proton and (ii) the chemical shift anisotropy (CSA) mechanism (see Wagner, 1993; Palmer et al., 1996). Chemical exchange on a millisecond time scale can also influence transverse relaxation (Szyperski et al., 1993; Orekhov et al., 1994). Rotational Brownian motion of the molecule in solution and intramolecular motions occurring on a pico-nanosecond time scale lead to fluctuations of the direction of the ^{1}H-^{15}N vector and/or symmetry axis of the CSA tensor with respect to the external magnetic field, causing the relaxation of ^{15}N nuclei. The fact that the symmetry axis of the CSA tensor and the direction of the backbone ^{1}H-^{15}N vector are nearly collinear allows one to describe two relaxation mechanisms by one correlation function. The correlation function can be rigorously factorized into the product of internal and overall terms under the conditions that the internal and overall motions are independent and the overall motion is isotropic. This factorization is also correct (but not rigorous) for anisotropic molecules (Lipari and Szabo, 1982). The observed relaxation rates and NOEs are determined by Fourier transformation of the correlation function (the spectral density J(ω)) evaluated at certain frequencies (Abragam, 1961). Therefore, the knowledge of the particular forms and rates of the overall and internal motions allows modeling of NMR relaxation.

Table 2. Characteristics of elementary processes of helix-coil transition

Process[a]	Description	Forward reaction rate
Helix propagation		
-**c**hh → -**h**hh c**c**hh → c**h**hh	New helical residue is added to the N-terminus of the helical region	k_F
hh**c**- → hh**h**- hh**c**c → hh**h**c	New helical residue is added to the C-terminus of the helical region	k_F
h**c**h → h**h**h	The coil residue, flanked on both sides by two helical residues, is converted to helical conformation	k_F
Helix nucleation		
-**c**c → -**h**c	*Step I* Formation of the first helical residue in the N-terminus of the polypeptide chain	$k_F \frac{v_{i+1}}{w_{i+1}}$
c**c**- → c**h**-	*Step I* Formation of the first helical residue in the C-terminus of the polypeptide chain	$k_F \frac{v_{i-1}}{w_{i-1}}$
c**c**c → c**h**c	*Step I* First helical residue is formed in the center of the coil region	$k_F \sqrt{\frac{v_{i-1}v_{i+1}}{w_{i-1}w_{i+1}}}$
-**c**hc → -**h**hc c**c**hc → c**h**hc	*Step II* The second helical residue is added at the N-terminus of the first helical residue	$k_F \frac{v_{i+1}}{w_{i+1}}$
ch**c**- →ch**h**- ch**c**c →ch**h**c	*Step II* The second helical residue is added at the C-terminus of the first helical residue	$k_F \frac{v_{i-1}}{w_{i-1}}$

[a] The *i*-th residue is underlined; the first and last residue are adjacent with a dash.

The influence of the helix-coil transition on NMR relaxation can be described within the frame of the discrete jump model for internal motions (King et al., 1978; King and Jardetzky, 1978; Wittebort and Szabo, 1978; Tropp, 1980). The application of this model to the helix-coil transition of 1–36BR requires several assumptions. First, since 1–36BR has a relatively high helix content and possesses well-defined α-helical structure in the 8–32 region, we assume that the overall rotation of the molecule is described as a rigid body diffusion and the overall and internal motions are independent. The second assumption is that in each of the states of the polypeptide chain a given backbone NH vector adopts a single direction in the molecular coordinate frame. Under the assumption that the internuclear vectors have constant length, one can use the following form of the correlation function of the internal motions:

$$C_I(t) = \langle P_2(\vec{\mu}(0)\vec{\mu}(t))\rangle$$

$$= \sum_{i=1}^{2^N} p_i^* \left\{ \sum_{j=1}^{2^N} p_j(t \mid \xi(0) = i) P_2(\vec{\mu}_i \vec{\mu}_j) \right\} \quad (9)$$

where $\vec{\mu}$ is the direction of the unit vector pointed along the ^{1}H-^{15}N bond in the molecular coordinate frame, $P_2(x) = 0.5(3x^2 - 1)$ is the second Legendre polynomial, p_i^* is the equilibrium population of the *i*-th state of the polypeptide chain, $p_j(t \mid \xi(0) = i)$ is the conditional probability for the system to be in state *j* at time *t* if at the initial moment it was in state *i*, the angular brackets mean averaging over the ensemble. The conditional probabilities $p_j(t \mid \xi(0) = i)$ can be calculated from Equations 7 and 8. Then Equation 9 can be rewritten as

$$C_I(t) = \sum_{i=1}^{2^N} p_i^* \left\{ \sum_{j=1}^{2^N} \sum_{k=1}^{2^N-1} c_k^{(\xi(0)=i)} x_{kj} e^{\lambda_k t} P_2(\vec{\mu}_i \vec{\mu}_j) \right\} + \sum_{i=1}^{2^N} \sum_{j=1}^{2^N} p_i^* p_j^* P_2(\vec{\mu}_i \vec{\mu}_j) \quad (10)$$

where $c_k^{(\xi(0)=i)}$ are the coefficients calculated from Equation 8 for each initial state *i* of the polypeptide chain. The last term in Equation 10 is equal to $C_I(\infty)$ and under the condition that all internal motions are faster than the overall rotation corresponds to the generalized order parameter. If the spectrum of correlation

times of the helix-coil transition is overlapping with the time scale of overall rotation, the observed order parameters have intermediate values.

Modeling of $C_I(t)$ for a given NH vector requires knowledge of the values of $P_2(\vec{\mu}_i\vec{\mu}_j)$ (see Equation 10), characterizing the relative directions of the vector in the molecular coordinate frame, for each pair of the states of the polypeptide chain. In this paper we use two different procedures for evaluation of $P_2(\vec{\mu}_i\vec{\mu}_j)$. In the first procedure, for a given NH vector we set $P_2(\vec{\mu}_i\vec{\mu}_j) = 1$ if in both the *i*-th and the *j*-th states of the polypeptide chain the corresponding residue is in a helical conformation. If the residue is in coil conformation at least in one of the *i*-th or the *j*-th states, $P_2(\vec{\mu}_i\vec{\mu}_j) = 0$. This procedure assumes that the direction of the NH vector in the molecular coordinate frame depends only on the conformation of its residue. The second procedure for evaluation of $P_2(\vec{\mu}_i\vec{\mu}_j)$ is aimed to account for kinked states of 1–36BR with several α-helical regions, expected due to the unstable central part of the peptide (see Pervushin et al., 1992; Nolde et al., 1997; Korzhnev et al., 1999). As in the first case we set $P_2(\vec{\mu}_i\vec{\mu}_j) = 0$ if at least in one of the two states the residue is in a coil conformation. If in both states the residue is helical, but at least in one of the states there are two or more helical regions within the peptide, we set $P_2(\vec{\mu}_i\vec{\mu}_j) = 0.5$. If in both states the residue is helical and there is only one helical region in the peptide we set $P_2(\vec{\mu}_i\vec{\mu}_j) = 1$.

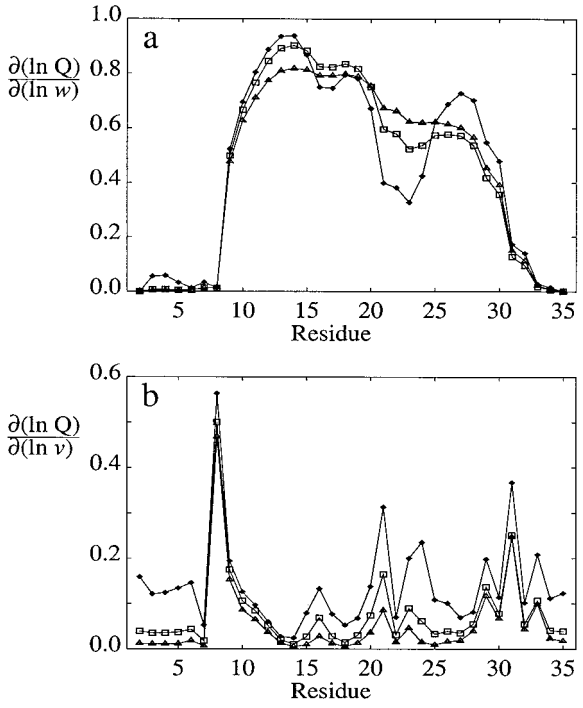

Figure 1. Probabilities of (a) *w*-weighting and (b) *v*-weighting for the residues of 1–36BR calculated with relative helix propensities of amino acids, determined from host-guest studies of short water-soluble peptides (Park et al., 1993). *w*-weighting of residue *i* means the formation of a $(CO)_{i-2}$–$(NH)_{i+2}$ hydrogen bond; *v*-weighting means that residue *i* terminates the helix region. Calculations are performed for different nucleation parameters: $\sigma = 10^{-4}$: triangles; $\sigma = 10^{-3}$: squares; $\sigma = 10^{-2}$: filled rhombs. The mean helix content in the region Pro8-Met32 is always equal to 0.6.

Results and discussion

Selection of amino acid propensities and nucleation parameter for calculations of the statistical weights of the states of 1–36BR.

Since transmembrane segment 1–36BR is composed mostly from nonpolar amino acids one might suggest that the propensities, determined from short monomeric α-helices in water would be suitable for modeling of 1–36BR in organic solvent. Indeed, the main factor determining the relative helix propensities of amino acids with nonpolar side chains is the loss of the side chain conformational entropy during α-helix formation (Lyu et al., 1990; Creamer and Rose, 1992). This factor is common for water and organic solutions. However, other factors, such as the hydrophobic effect of burial of nonpolar surfaces of side chains and the formation of side chain-backbone hydrogen bonds (Chakrabartty and Baldwin, 1995) can lead to some differences between the relative helix propensities in water and in organic solvents.

Several sets of relative α-helix propensities of amino acids were tested to select proper model parameters for calculations of the statistical weights of the states of 1–36BR. In particular, two most complete sets (Table 1) were selected among those obtained by the host-guest technique for short water-soluble monomeric peptides and coiled-coil systems (Lyu et al., 1990; O'Neil and DeGardo, 1990; Padmanabhan et al., 1990; Chakrabartty et al., 1991). The selected sets of relative helix propensities exhibit practically identical profiles of mean residual helicity (Figure 1). To reach a mean helix content of 0.6, expected for region Pro8-Met32 in a weakly polar organic mixture (see Korzhnev et al., 1999), the helix propensities have to be scaled by a factor 2.9–3.5 with respect to those obtained in water. For all values of the helix nucleation parameter ($\sigma = 10^{-4}, 10^{-3}$ and

10^{-2}) the α-helix position in 1–36BR in the organic mixture (Pervushin et al., 1992) was well reproduced. In all cases the most probable position of the α-helix is Glu9-Lys30 (Figure 1a) with the terminal residues Pro8 and Gly31 (Figure 1b). The regions Gly16-Thr17 and Gly21-Thr24 with enhanced probabilities of helix breaks (Figure 1b) coincide with the regions of the formation of metastable π-bulges observed by Korzhnev et al. (1999) in the molecular dynamics simulations of 1–36BR in weakly polar solvent. The smoothness of the helicity profile and probability of α-helix breaks are determined by nucleation parameter σ. The value $\sigma = 10^{-4}$ gives a smooth profile with helix content decreasing in the C-terminal part of the Pro8-Met32 region (Figure 1a). The value $\sigma = 10^{-3}$ provides a similar helicity profile with poorly defined minima near Gly16-Thr17 and Gly23-Thr24 (Figure 1a). The calculations with $\sigma = 10^{-2}$ clearly determine two stable parts of the α-helix separated by the region Gly21-Thr24 with relatively low helical content (Figure 1a) and high probability of α-helix break (Figure 1b). In the stable Trp10-Met20 part the probability of a helix break is slightly increased near Gly16 and Thr17. The existence of the metastable Gly21-Thr24 fragment, separating two helical regions, is in agreement with the enhanced deuterium exchange of the backbone amides of residues Gly21-Thr24 of 1–36BR in organic mixture (Pervushin et al., 1992). NMR study of 1–36BR in chloroform/methanol mixture (Pervushin et al., 1992) reveals two consecutive γ-turns of 2_7-helix in the N-terminal part (residues 1–7) of 1–36BR. The reverse turns might serve as intermediates of α-helix nucleation (Tobias and Brooks, 1991). The considerable probability ($\sim$ 0.1) of the formation of α-helix turn near the residues Gln3-Thr5 profiles were observed only in calculations with $\sigma = 10^{-2}$ (Figure 1a). Thus, the nucleation parameter $\sigma = 10^{-2}$ and the relative helix propensities, determined from host-guest studies of short monomeric peptides in water (with appropriate scaling) provide good agreement with the experimental NMR data on the α-helix location and on exchange rates of amide protons of 1–36BR in chloroform/methanol mixture (Pervushin et al., 1992) and with the MD simulations of 1–36BR in weakly polar media (Korzhnev et al., 1999). The appropriately scaled helix propensities of Park et al. (1993) (see Table 1) were selected for calculations of the statistical weights of 1–36BR states in the kinetic modeling.

The obtained results suggest that the helix-coil transition in weakly polar chloroform/methanol mixture is characterized by (i) uniform increase ($\sim$3–3.5 times) of the absolute values of helix propensities of amino acids with respect to those observed for water-soluble peptides and (ii) high $\sim 10^{-2}$ nucleation parameter σ (10^{-2} is the upper bound for s, estimated by Zimm and Bragg (1959)). The increase of the absolute values of intrinsic helix propensities is expected due to the strengthening of short-range electrostatic interactions (in particular hydrogen bonding) in a weakly polar environment. The increase of nucleation parameter σ is presumably caused by the absence of strong solvent concurrence for hydrogen bonding in the coil state in a weakly polar medium.

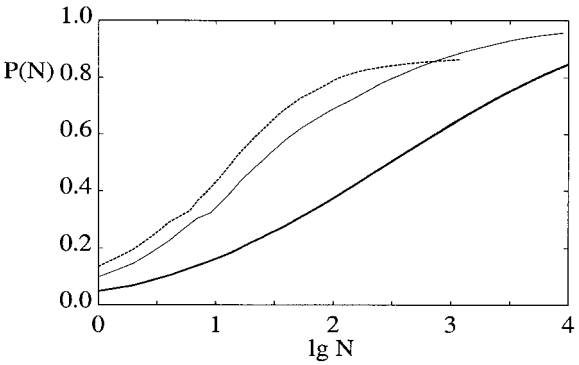

Figure 2. Total weight of the N most populated states of 8–33BR versus the number of states calculated for different nucleation parameters: $\sigma = 10^{-4}$: dashed line; $\sigma = 10^{-3}$: thin solid line; $\sigma = 10^{-2}$: bold solid line.

Selection of the states of 1–36BR for kinetic modeling

It is obvious that the solution of the system of 2^N kinetic equations is a computional challenge for peptides with more than 10 residues (our computers allow to solve systems of $\sim 10^3$–10^4 rate equations). To reduce the number of states in the kinetic modeling the calculations were performed for the Pro8-Gly33 part of 1–36BR. It is notable that the profile of mean residual helicity, calculated without accounting for terminal parts pGln1-Arg7 and Val34-Asp36, practically coincides with those calculated for the whole peptide. Even for the Pro8-Gly33 region there are 2^{26} or 6.7×10^7 states, which renders impossible the numerical solution of the system of rate equations 4. However, if the majority of low-populated states are excluded, the calculations can be substantially simplified. Indeed, the first 10^3 most populated states of 8–33BR account for ∼60–70% of the total weight of the states at $\sigma = 10^{-2}$ and ∼90% at $\sigma = 10^{-3}$ or $\sigma = 10^{-4}$ (Figure 2).

Table 3. Populations of the states with the given number of helical regions within 8–33BR, calculated for different nucleation parameters σ

Number of helical regions	$\sigma = 10^{-2}$	$\sigma = 10^{-3}$	$\sigma = 10^{-4}$
0	0.002	0.047	0.16
1	0.43	0.85	0.83
2	0.52	0.10	0.01
3	0.04	0.001	0

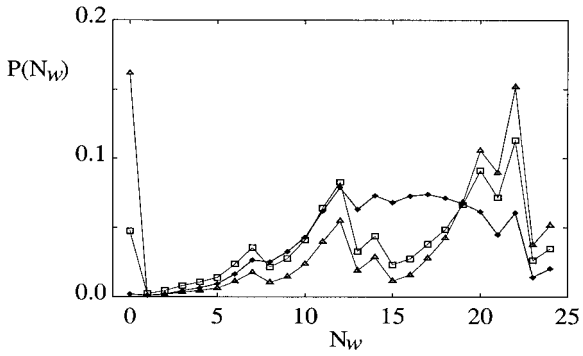

Figure 3. Probabilities of the states with a different number of α-helical hydrogen bonds (or number of *w*-weighted residues) N_w within 8–33BR calculated for different nucleation parameters: $\sigma = 10^{-4}$: triangles; $\sigma = 10^{-3}$: squares; $\sigma = 10^{-2}$: filled rhombs.

Kinetic modeling of short water-soluble homopeptides is usually carried out using the 'one-sequential' approximation (Schellman, 1958) in which states with one non-perturbed helical region and the all-coil state are allowed (see Thompson et al., 1997). The consideration of a heteropeptide, such as 8–33BR, in organic solvent is complicated since the states with more than one helical region within the peptide can be highly populated. This is caused by (i) existence of the helix breakers (Gly and Thr) in the central part of the peptide and (ii) increase of the nucleation parameter σ, determining the length of helix regions (the mean length of a helical region is proportional to $\sigma^{-1/2}$). Indeed, the calculations with $\sigma = 10^{-2}$ show that the total population of the states with more than one helical region within 8–33BR exceeds 0.5; in the case of $\sigma = 10^{-3}$ this population is ∼0.1; in the case of $\sigma = 10^{-4}$ the population is 0.01, allowing the 'one-sequential' approximation (Table 3).

There are common criteria for selection of the states, required to reproduce the cooperative nature of the helix-coil transition. The cooperativity of the transition is determined by nucleation parameter $\sigma \ll 1$ and implies that there are two groups of the most populated states: the all-coil state and the states close to all-helix. In the limit of $\sigma \to 0$ the transition between all-coil and all-helix states occurs without significantly populated intermediates. For proper kinetics modeling (i) the minimal set of selected intermediates must account for almost all total weight of the states and (ii) the connectivities between the selected states (in particular, between all-coil and helical states) have to be provided.

For nucleation parameters $\sigma = 10^{-4}$ and $\sigma = 10^{-3}$ kinetic modeling was performed for the states with statistical weights higher than the weights of helix nuclei (v^2) – the maximal cutoff required to provide the connectivity between the all-coil state and helical states. For these nucleation parameters the most populated state is all-coil (populations 0.05 for $\sigma = 10^{-3}$ and 0.16 for $\sigma = 10^{-4}$) (see Figure 3 and Table 3). The most probable number of *w*-weighted residues (20 or 22) in 8–33BR is close to the maximal available length of the helix (Figure 3), while the states with intermediate numbers of α-helical hydrogen bonds, i.e. with a maximal number of realizations (the number of states with k helical residues in the N-residual peptide – C_N^k is maximal for $k \cong N/2$), have low populations. For these reasons the v^2-criterion provides a relatively low number of states (∼900 for $\sigma = 10^{-4}$ and ∼1800 for $\sigma = 10^{-3}$) accounting for more than 90% of the total weight of the states.

For nucleation parameter $\sigma = 10^{-2}$ the selection according to the v^2-criterion is impossible because the partially folded states with an intermediate number of α-helical hydrogen bonds have relatively high populations. Indeed, there are $\sim 2 \times 10^4$ states with statistical weights higher than the weight of helix nuclei. However, for $\sigma = 10^{-2}$ the weight of the all-coil state is negligibly small (Figure 3 and Table 3) and we cannot separate the states into the two most populated groups. In this case the dynamics can be considered within the group of helical states. Therefore, the kinetic modeling is performed with the 1500 most populated states, accounting for ∼70% of the total weight of the states.

Results of the kinetic modeling: NMR correlation functions for backbone NH vectors

Correlation functions of the internal motions $C_I(t)$ for ^{1}H-^{15}N vectors of 1–36BR can be represented by multiexponential decays (Equation 10). The estimates of the order parameters of the backbone NH vectors can be obtained from the decays of correla-

tion functions $C_I(t)$ in the particular time intervals. The values of the correlation function at 1–100 ps approximately correspond to the order parameter of fast internal motions (S_f^2). The decay of $C_I(t)$ up to ~10 ns provides rough estimates of the generalized order parameter ($S^2 = S_f^2 S_s^2$) in the molecules with an overall rotation correlation time (τ_R) of several nanoseconds. Using these simple approximations for S^2 and S_f^2 one can easily get the estimates for order parameters of nanosecond motions S_s^2. In principle, at this stage one can also account for the effects of fast (femto-picosecond) vibrational motions, which are not considered in our model, but which can affect the order parameters S_f^2. The order parameters S_f^2 of these motions are high (~0.8–0.9) and practically independent of the secondary structure of proteins (Palmer and Case, 1992; Orekhov et al., 1995a).

The analysis of the eigenvalues (λ_i) of the rate matrix (see theoretical part) reveals a wide spectrum of correlation times ($\tau_i = -1/\lambda_i$) of the helix-coil transition of 1–36BR (Figure 4). The correlation times vary from 10^{-11} s to 10^{-6} s. On the pico-nanosecond time scale the spectrum is practically continuous. In contrast, between tens of nanoseconds and microseconds there are only several discrete correlation times. The weights of the exponential terms in C_I(t) (Equation 10) are analyzed using distribution function F(t), which is the sum of the weights of exponents with correlation times $\tau_i < t$. It is notable that $F(\infty) = 1 - C_I(\infty)$. Figure 4 shows distribution functions F(t) of selected backbone NH-groups, calculated for different nucleation parameters and $P_2(\vec{\mu}_i \vec{\mu}_j)$, accounting for the kinked states of the helix (see theoretical part). Calculations with $\sigma = 10^{-3}$ and 10^{-4} reveal two distinct groups of exponents with maximal weights in C_I(t) (Figure 4b,c). The first, 'slow' group includes several exponential terms with correlation times ranging from hundreds of nanoseconds to microseconds and characterizes the passage over the nucleation free energy barrier (transition between all-coil state and the group of helical states). The second, 'fast' group includes exponents with pico- and nanosecond correlation times and characterizes the equilibration of the helical species. It is notable that the existence of two groups of exponential terms is inherent for processes of the helix-coil equilibration and can be observed experimentally. In particular, in a kinetic study of a short alanine-based peptide, Thompson et al. (1997) observed two-exponential decay for the fraction of N-terminal residues following a laser-induced temperature jump and monitored by fluorescence probe. With the increase of nucleation parameter σ the weights of the exponents from the 'fast' group increase (Figure 4). In contrast, the weights of exponential terms from the 'slow' group decrease and their correlation times become faster. The decrease of the weights is proportional to the decrease of the population of the all-coil state with the increase of σ. Indeed, in calculations with $\sigma = 10^{-2}$, where the weight of the all-coil state is negligible, the maximal correlation time does not exceed 100 ns and the correlation functions C_I(t)

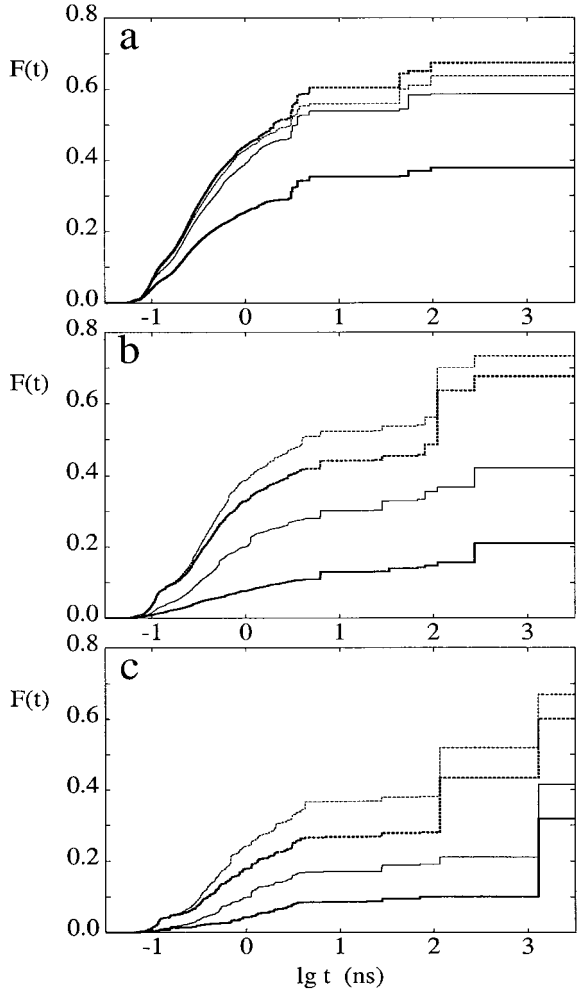

Figure 4. Distribution functions F(t), characterizing the weights of exponents with correlation times $\tau_i < t$ in multiexponential correlation function C_I(t), calculated taking into account kinked states of the helix for different values of nucleation parameter: (a) $\sigma = 10^{-2}$; (b) $\sigma = 10^{-3}$; (c) $\sigma = 10^{-4}$. The distribution functions F(t) are plotted for four selected residues: Ala14: bold solid line; Met20: thin solid line; Leu25: bold dashed line; Leu28: thin dashed line.

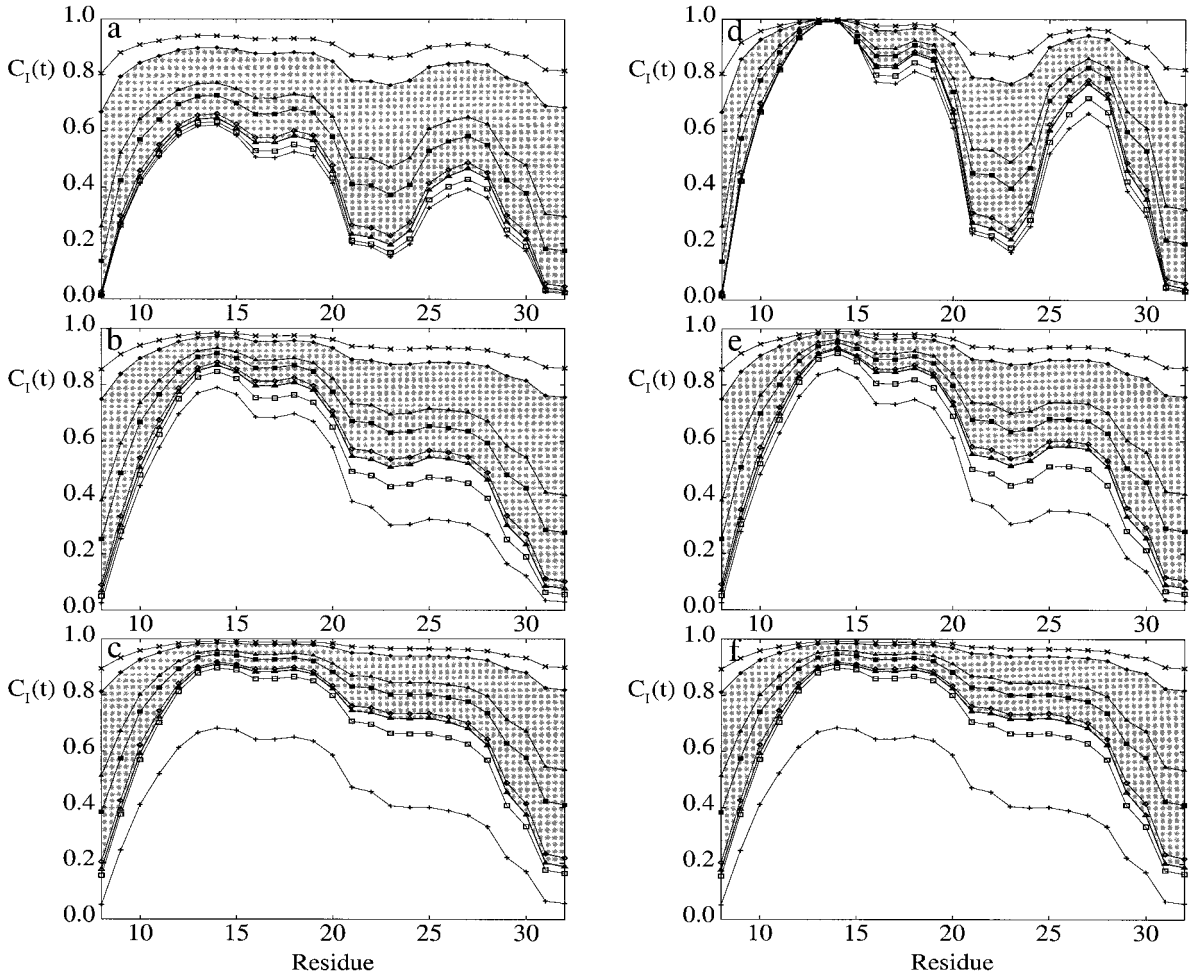

Figure 5. Correlation functions $C_I(t)$ of the backbone NH vectors of 8–33BR calculated with (a–c) and without (d–f) accounting for the kinked states of the helix for different values of nucleation parameter: (a, d) $\sigma = 10^{-2}$; (b, e) $\sigma = 10^{-3}$; (c, f) $\sigma = 10^{-4}$. The values of $C_I(t)$ are sampled at the following times (from top to bottom on all plots): 50 ps; 100 ps; 500 ps; 1 ns; 5 ns; 10 ns; 50 ns; $t = \infty$. Drop of the correlation functions $C_I(t)$ between 100 ps and 10 ns is filled in gray. Drop of correlation functions up to ~100 ps and ~10 ns provides rough estimates of S_f^2 and $S^2 = S_f^2 S_s^2$, respectively.

are determined only by the 'fast' group of exponents (Figure 4a).

The drop of the correlation functions $C_I(t)$ in the interval 0–10 ns (Figure 5), responsible for generalized order parameters S^2 of ^{1}H-^{15}N vectors, is mostly determined by the 'fast' group of exponents. The increase of the weights of exponential terms from this group at nucleation parameter $\sigma \sim 10^{-2}$ ensures low order parameters of nanosecond motions S_s^2 for 8–33BR (see Figure 5a,d). In the cases of $\sigma = 10^{-3}$ (Figure 5b,e) and $\sigma = 10^{-4}$ (Figure 5c,f) the expected order parameters S_s^2 are higher due to decrease of the weight of 'fast' and increase of the weight of 'slow' groups of exponents.

The comparison of correlation functions, calculated using different methods for assignment of $P_2(\vec{\mu}_i \vec{\mu}_j)$ (see theoretical part), shows (Figure 5) that it is necessary to account for kinked states of the helix in order to explain low and *uniform* (over 1–36BR) order parameters S_s^2 observed by Orekhov et al. (1999). Indeed, in weakly polar solvent with high nucleation parameter $\sigma = 10^{-2}$ the percentage of the states with more than one helical region within 8–33BR is ~56% (Table 3). The drop of correlation functions, calculated at $\sigma = 10^{-2}$ without accounting for these states, is not uniform over the peptide (Figure 5d). In this case the expected order parameters S_s^2 vary from ~0.4 for Gly21-Thr24 to 1.0 for Leu13-Ala14. Tak-

ing into account the states with more than one helical region significantly improves the agreement with the experimental order parameters S_s^2 (∼0.5–0.6). The expected order parameters S_s^2 (0.5–0.7 for Trp10-Met20; ∼0.4 for Gly21-Thr24 and ∼0.5 for Leu25-Leu28) are practically uniform over the peptide (see Figure 5a) and agree well with those observed by Orekhov et al. (1999). The percentage of the kinked states for lower nucleation parameters σ is small (∼10% for $\sigma = 10^{-3}$ and ∼1% for $\sigma = 10^{-4}$) (Table 3) and the correlation functions calculated with (Figure 5b,c) and without (Figure 5e,f) account of kinked states are practically identical. The minimal order parameters S_s^2 expected in the region Trp10-Leu28 are higher than 0.7–0.8 for $\sigma = 10^{-3}$ and 0.8–0.9 for $\sigma = 10^{-4}$ and, therefore, do not agree with experimental values.

The values of S_s^2 obtained from NMR relaxation data depend on (i) distribution of the correlation times of the intramolecular processes and the weights of corresponding exponential terms in $C_I(t)$, (ii) parameters of overall rotation of the molecule and (iii) the particular set of experimental data used for extraction of order parameters and correlation times. Thus, in principle, a comprehensive analysis within the frame of a particular model has to include calculations of model relaxation data followed by extraction of order parameters using standard methods of relaxation data analysis (see e.g. Orekhov et al., 1995b). The procedure used in this paper for modeling of the NMR relaxation can provide qualitative results only. Certainly, some states of the polypeptide chain (e.g. all-coil state) are complex and in these states a given NH vector can adopt a number of directions. Also, we used an illustrative rather than an exact method for assignment of the NH vector directions. Strictly speaking, the flexible N- and C-terminal parts and the presence of kinked states do not allow us to describe overall rotation of 1–36BR as a rigid body diffusion and the internal and overall motions cannot be regarded as independent. Because of these reasons we do not perform further calculations of relaxation rates and NOEs for a direct comparison with the experimental data. However, the present analysis of the correlation functions is sufficient to establish the origin of the high-amplitude nanosecond motions in 1–36BR observable by NMR and to explain the uniform (over the α-helix) order parameters of these motions.

In summary, the main results of the present modeling are the following: 1. Relative helix propensities of amino acids, measured by the host-guest technique in short water-soluble peptides (Park et al. 1993; Chakrabartty and Baldwin, 1995), are suitable for modeling of transmembrane α-helix in a weakly polar medium. The helix-coil transition in a weakly polar medium is characterized by high nucleation parameter $\sigma \sim 10^{-2}$ and uniform increase (∼3–3.5 times) of helix propensities with respect to those obtained for water-soluble peptides. 2. The helix-coil transition of 1–36BR is characterized by a wide spectrum of correlation times ranging from 10^{-11} s to 10^{-6} s. There are two distinct groups of exponential terms in multiexponential correlation functions $C_I(t)$ of backbone NH vectors: 'fast' (pico-nanoseconds) and 'slow' (submicroseconds). In the weakly polar medium with $\sigma \sim 10^{-2}$ the exponential terms from the 'fast' group dominate in $C_I(t)$. 3. The origin of the uniformly low order parameters of nanosecond motions in 1–36BR (Orekhov et al., 1999) is an exchange between the kinked states of 1–36BR. In the weakly polar medium with $\sigma \sim 10^{-2}$ the percentage of the kinked states with more than one helical region in 1–36BR exceeds 50%.

Conclusions

The motional model of 1–36BR, proposed in this paper, considers the effect of helix-coil transition on ^{1}H-^{15}N NMR relaxation of the backbone NH groups of 1–36BR. The proposed kinetic model has no limitations on the time scale of studied motions, inherent for molecular dynamics simulations, and clearly determines the origin of nanosecond internal motions in the isolated α-helical fragment 1–36BR. The kinked states of the α-helix, leading to uniformly low order parameters of nanosecond motions of 1–36BR (Orekhov et al., 1999) are caused (i) by the low polarity of the solvent system used (in particular, for high nucleation constant $\sigma = 10^{-2}$) and (ii) by the presence of strong helix breakers Gly and Thr, determining the most probable positions of helix breaks within 1–36BR. The predicted positions of helix breaks coincide with the regions of α-helix distortions, termed as π-bulges, observed in MD simulations of 1–36BR in weakly polar medium (Korzhnev et al., 1999). During the formation of π-bulges the α-helix becomes shorter and π-bulge connected parts of the helix can turn with respect to each other. It is interesting to note that the mutation of helix breakers (e.g. Gly, Thr as well as Pro, Ile, Val) can often impair the function of membrane proteins (Deber and Li, 1995 and references cited therein). The above discussed results as well as the results of Deber and Li (1995), Li et al. (1996) and Li and Deber (1992)

indicate the specific role of α-helix breakers in providing the conformational dynamics required for the functioning of membrane proteins.

Acknowledgements

We thank Dr I.L. Barsukov for careful reading of the manuscript. This work was supported by Russian Foundation for Basic Research grants 96-04-00054, 96-04-50893 and by ISSEP grants a97-969 and a98-2221.

References

Abragam, A. (1961) *Principles of Nuclear Magnetism*, Clarendon press, Oxford.
Chakrabartty, A. and Baldwin, R.L. (1995) *Adv. Protein Chem.*, **46**, 141–176.
Chakrabartty, A., Schellman, J.A. and Baldwin, R.L. (1991) *Nature*, **351**, 586–588.
Creamer, T.P. and Rose, G.D. (1992) *Proc. Natl. Acad. Sci. USA*, **89**, 5937–5941.
Dagget, V. and Levitt, M. (1992) *J. Mol. Biol.*, **233**, 1121–1138.
Deber, C.M. and Li, S.C. (1995) *Biopolymers*, **37**, 295–318.
Doig, A.J., Chakrabartty, A., Kingler, T.M. and Baldwin, R.L. (1994) *Biochemistry*, **33**, 3396–3403.
King, R. and Jardetzky, O. (1978) *Chem. Phys. Lett.*, **55**, 15–18.
King, R., Maas, R., Gassner, M., Nanda, R.K., Conover, W.W. and Jardetzky, O. (1978) *Biophys. J.*, **6**, 103–117.
Korzhnev, D.M., Orekhov, V.Yu., Arseniev, A.S., Gratias, R. and Kessler, H. (1999) *J. Phys. Chem. B*, **103**, 7036–7043.
Li, S.C. and Deber, C.M. (1992) *FEBS Lett.*, **311**, 217–220.
Li, S.C., Goto, N.K., Williams, K.A. and Deber, C.M. (1996) *Proc. Natl. Acad. Sci. USA*, **93**, 6676–6681.
Lifson, S. and Roig, A. (1961) *J. Chem. Phys.*, **34**, 1963–1974.
Lipari, G. and Szabo, A. (1982) *J. Am. Chem. Soc.*, **104**, 4546–4559.
Lyu, P.C., Liff, M.I., Marky, L.A. and Kallenbach, N.R. (1990) *Science*, **250**, 669–673.
Nolde, D.E., Arseniev, A.S., Vergoten, G. and Efremov, R.G. (1997) *J. Biomol. Struct. Dyn.*, **15**, 1–18.
O'Neil, K.T. and DeGardo, W.F. (1990) *Science*, **250**, 646–651.
Orekhov, V.Yu., Pervushin, K.V. and Arseniev, A.S. (1994) *Eur. J. Biochem.*, **219**, 887–896.
Orekhov, V.Yu., Pervushin, K.V., Korzhnev, D.M. and Arseniev, A.S. (1995a) *J. Biomol. NMR*, **6**, 113–122.
Orekhov, V.Yu., Nolde, D.E., Golovanov, A.P., Korzhnev, D.M. and Arseniev, A.S. (1995b) *Appl. Magn. Reson.*, **9**, 581–588.
Orekhov, V.Yu., Korzhnev, D.M., Diercks, T., Kessler, H. and Arseniev, A.S. (1999) *J. Biomol. NMR*, **14**, 345–356.
Padmanabhan, S., Marqusee, S., Ridgeway, T., Laue, T. and Baldwin, R. (1990) *Nature*, **344**, 268–270.
Palmer, A.G and Case, D.A. (1992) *J. Am. Chem. Soc.*, **114**, 9059–9067.
Palmer, A.G., Williams, J. and McDermott, A. (1996) *J. Phys. Chem.*, **100**, 13293–13310.
Park, S.H., Shalongo, W. and Stellwagen, E. (1993) *Biochemistry*, **32**, 7084–7053.
Pervushin, K.V., Sobol, A.G., Musina, L.Yu., Abdulaeva, G.V. and Arseniev, A.S. (1992) *Mol. Biol. (Russia)*, **26**, 920–933.
Qian, H. and Schellman, J.A. (1992) *J. Phys. Chem.*, **96**, 3987–3994.
Schellman, J.A. (1958) *J. Phys. Chem.*, **62**, 1485–1494.
Scholtz, J.M. and Baldwin, R.L. (1992) *Annu. Rev. Biophys. Biomol. Struct.*, **21**, 95–118.
Schwartz, G. (1965) *J. Mol. Biol.*, **11**, 64–77.
Schwartz, G. (1968) *Biopolymers*, **6**, 873–897.
Schwartz, G. and Seelig, J. (1968) *Biopolymers*, **6**, 1263–1277.
Szyperski, T., Luginbuhl, P., Otting, G., Guntert, P. and Wüthrich, K. (1993) *J. Biomol. NMR*, **3**, 151–164.
Thompson, P.A., Eaton, W.A. and Hofrichter, J. (1997) *Biochemistry*, **36**, 9200–9210.
Tobias, D.J. and Brooks, C.L. (1991) *Biochemistry*, **30**, 6059–6070.
Tropp, J. (1980) *J. Chem. Phys.*, **72**, 6035–6043.
Wagner, G. (1993) *Curr. Opin. Struct. Biol.*, **3**, 748–754.
Williams, S., Causgrove, T.P., Gilmanshin, R., Fang, K.S., Callender, R.H., Woodruff, H.W. and Dyer, R.B. (1996) *Biochemistry*, **35**, 691–697.
Wittebort, R.J. and Szabo, A. (1978) *J. Chem. Phys.*, **69**, 1722–1736.
Zana, R. (1975) *Biopolymers*, **14**, 2425–2428.
Zimm, B.H. and Bragg, J.K. (1959) *J. Chem. Phys.*, **31**, 526–535.